JACS
JOURNAL OF THE AMERICAN CHEMICAL SOCIETY
Communication
pubs.acs.org/JACS

Surface Control of Alkyl Chain Conformations and 2D Chiral Amplification

Nadine Hauptmann,[†] Katharina Scheil,[†] Thiruvancheril G. Gopakumar,*[,†] Franziska L. Otte,[‡] Christian Schütt,[‡] Rainer Herges,[‡] and Richard Berndt[†]

[†]Institut für Experimentelle und Angewandte Physik, Christian-Albrechts-Universität zu Kiel, 24098 Kiel, Germany
[‡]Otto-Diels-Institut für Organische Chemie, Christian-Albrechts-Universität zu Kiel, Otto-Hahn-Platz 4, 24098 Kiel, Germany

Supporting Information

ABSTRACT: Trioctyl-functionalized triazatriangulenium (trioctyl-TATA) deposited on Au(111) and Ag(111) surfaces by electrospray ionization was investigated using low-temperature scanning tunneling microscopy. The molecule surprisingly adsorbs with gauche rather than anti conformations of the octyl groups. We observed chiral amplification in the islands. Only one of the eight possible configurations of the octyl groups was found in homochiral hexagonal networks. Quantum-chemical calculations confirmed and explained the preference for the gauche conformations of adsorbed trioctyl-TATA.

Alkanes and molecules with alkyl chains are the basic building blocks of lipids, surfactants, and liquid crystals. The crystallinity of these materials in bulk form is limited by the large number of possible conformations. In the gas phase, the anti conformation of alkanes is usually more stable than the gauche conformation.[1] For pentane and larger *n*-alkanes at room temperature, however, instead of the all-anti-configured alkane chain (anti form), structures that include one or more gauche conformations are the predominant species because they are more probable for statistical reasons.[2,3] Even near 0 K, long alkane chains (>17 C atoms) are not in the anti form. The global minimum is a chain with four gauche conformations that fold the alkane into a hairpin shape. The structure is stabilized by the dispersion self-interaction of the two anti-configured ends.[4]

Similarly, on surfaces, conformations of alkane chains that maximize intermolecular dispersion interactions and thus promote crystallization are selected. A number of reports on alkyl substituents[5] and alkane chains[6] in ultrathin layers have shown that adjacent alkyl chains align parallel to each other and the surface. In these layers, the anti form is preferred, leading to close-packed lamellar structures. The zigzag orientation reduces the steric hindrance between H atoms of the methylene groups in adjacent chains and maximizes van der Waals contact. Indications of first-layer molecules in the energetically less favorable gauche conformation are scarce. While vibrational spectroscopy suggested that they may occur as defects in layers of molecules in an anti form,[7] imaging of ordered networks with gauche conformations was not feasible.[8] However, gauche conformations in multilayers have been observed by vibrational spectroscopy[7,9,10] and surface scattering methods.[8,11] Alkyl-substituted achiral molecules may form chiral domains at solid−liquid interfaces[5a,h,i,12] and under ambient conditions.[5b,6a,8]

At ambient temperatures, molecular mobility occurs on Au and Ag surfaces. As a result, scanning tunneling microscopy (STM) often resolves only compact molecular patterns. To get further insight into the adsorption geometry of alkyl chains on surfaces, low-temperature STM measurements in an ultrahigh vacuum (UHV) environment are needed. Because of the low thermal stability of molecules with long alkyl chains, standard sublimation methods for UHV preparation are not feasible. The majority of the crystalline ultrathin films of pure alkanes,[6a−d,13] alkyl chains with functional groups (e.g., alcohols,[5d,6a,14,15] acids,[6a] halides,[14,16] thiols,[17] and nitriles[14]), and alkyl-functionalized molecules[5b−i,18] have therefore been prepared and analyzed at liquid−solid interfaces. Vacuum-deposited structures on surfaces are scarce.[7,8,19]

To circumvent the problem of low thermal stability, we used a home-built electrospray ion source[20] to deposit octyl-functionalized triazatriangulenium[21] (trioctyl-TATA; Figure 1c) in UHV. STM imaging was performed on Au(111) in situ at ∼5 K. In the gas phase, the anti form of the octyl chains is most favorable according to density functional theory (DFT) (Figure 1a,b). Surprisingly, we observed that the molecules adsorb in the gauche form (at least one gauche conformation in each octyl chain; Figure 1c). The exocyclic bond between C1 and C2 in the octyl chain cannot lie parallel to the ring plane as in the case of trioctylamine (TOA),[22] as steric hindrance between the C2 protons and the H atom of the neighboring benzene ring forces it to point upward. As a result, the octyl chains grow away from the molecular plane (cf. Figure 1a,b), and their interaction with the surface is weak. To regain contact with the surface, a gauche conformation within the octyl chain is needed, giving rise to a bent geometry. Thus, molecules are either C_3-symmetric (all octyl groups oriented clockwise or anticlockwise) or C_1-symmetric (one octyl group oriented differently from the others). Hence, the molecules become chiral on the surface. At higher coverages, homochiral hexagonal islands were observed; their cores contained only C_3-symmetric molecules, whereas molecules at their perimeters could also be C_1-symmetric. This molecular arrangement is attributed to more favorable steric interactions in enantiopure islands. We made closely related observations for trioctyl-TATA networks on Ag(111).

Au(111) and Ag(111) substrates were cleaned by Ar^+ sputtering and annealing. Trioctyl-TATA (as its BF_4^- salt) was

Received: April 11, 2013
Published: June 1, 2013

   dx.doi.org/10.1021/ja4036187 | J. Am. Chem. Soc. 2013, 135, 8814−8817

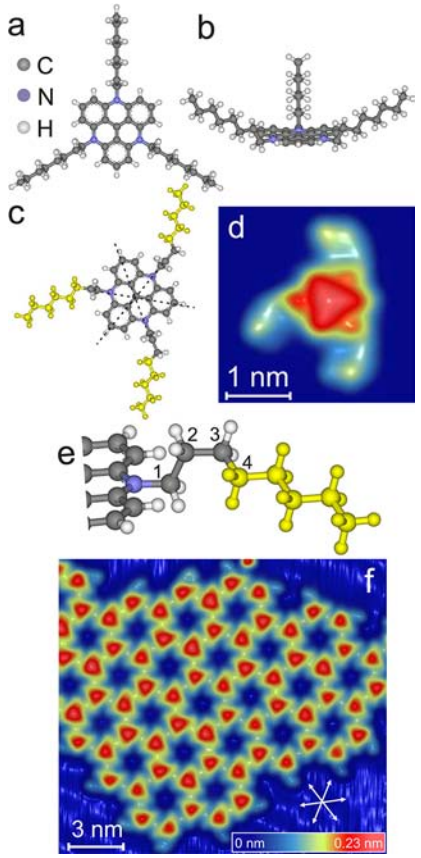

Figure 1. Calculated gas-phase structure of trioctyl-TATA in the anti form: (a) top view; (b) side view. (c) Model of trioctyl-TATA in the gauche form. The twofold axes of the triangular TATA center are marked by dashed lines. The structure of tripropyl-TATA on a Au cluster (not shown) was optimized using DFT (for details, see the text). To complete the octyl chains, an all-anti *n*-pentyl chain (yellow) was added to C3 in each chain. (d) Pseudo-three-dimensional (pseudo-3D)-illuminated constant-current STM topograph (100 mV, 100 pA) of a single trioctyl-TATA molecule adsorbed on Au(111). (e) Magnified octyl group of the model in (c). C1−C4 are discussed in the text. (f) Pseudo-3D-illuminated STM topograph (53 mV, 42 pA) of a self-assembled island of trioctyl-TATA on Au(111). One of the compact directions of Au(111) is marked.

dissolved in methanol ($\sim 10^{-6}$ M) and sprayed onto the substrate in positive-ion mode at ~5.1 kV at room temperature in UHV. While the cation of trioctyl-TATA was deposited, the molecules may be neutralized immediately during adsorption onto the metal substrate.

First, an isolated trioctyl-TATA molecule on Au(111) is addressed (Figure 1d). The threefold-symmetric TATA core and the three anchoring octyl groups are clearly discernible and can be compared with the optimized geometry obtained using DFT as discussed below (Figure 1c). TATA is adsorbed parallel to the substrate, as at solid−liquid interfaces.[18,23] The octyl groups appear as arcs, indicating that at least one methylene group is adsorbed with a gauche conformation rather than in the anti form as recently reported for TOA adsorbed on Au(111).[22]

To analyze the preference for the gauche form, DFT calculations on tripropyl-TATA adsorbed on a Au cluster (170 Au atoms in four layers with D_{3d} symmetry) as a model system were performed at the PBE/SV(P) level of theory.[24] The Grimme D3 parameters for dispersion interactions[25] were included using TURBOMOLE 6.2.[26] A gold cluster model was chosen to compare calculations for single molecules in the gas phase and on the surface at the same level of theory (for further details, see the Supporting Information). After the optimization of tripropyl-TATA, the propyl chains were lengthened to octyl chains and optimized at the PBE/SV(P) level.

The optimized geometry of trioctyl-TATA is shown in Figure 1c (C, gray; N, blue; H, white; substrate not shown). The N−C1 bond is not parallel to the surface because of steric interactions, as described above. The two C1 protons are oriented toward the surface, so the C1−C2 bond points upward (Figure 1e), and C3 is at nearly the same height as C2. The fourth methylene group (C4) can be attached in such a way that the chain points either upward (anti conformation) or sideways (gauche conformation). The gauche conformation is more favorable because it brings the alkyl chain back into contact with the surface and the adsorption energy increases with the length of the adsorbed alkyl chain.[27], The remaining three methylene groups and the terminal methyl group (yellow in Figure 1e) are in contact with the surface if they are in the anti conformation.

The lateral dimensions of the model with the gauche form agrees well with those measured in the experiment. The distance between the terminal methyl group and the center of molecule extracted from the model (~1.21 nm) compares well with the experimental value (~1.2 nm; Figure 1d). The conformation of the octyl chains in our low-temperature experiment deviates from the vertical orientation suggested for close-packed layers of trioctyl-TATA on Au(111) in solution.[18,23a] This discrepancy may be due to the modified interactions in a solvent as well as the widely different temperatures.

At a nominal coverage of 0.1 molecule/nm^2, almost all of the trioctyl-TATA molecules are arranged in islands with a honeycomb pattern (Figure 1f) at an intermolecular distance of ~1.8 nm. The TATA molecular axes (Figure 1c, dashed lines) are oriented along the compact directions of Au(111) (Figure 1f, white arrows). This minimizes the mismatch between the distances of the N atoms of TATA (4.86 Å) and the atomic next-nearest-neighbor distance on Au(111) to only 3%, allowing N to adsorb at equivalent sites (see section S2 in the SI).[23a]

High-resolution STM topographs of trioctyl-TATA islands (Figure 2a,b) revealed that the octyl groups of every molecule within the island exhibit the gauche form. Corresponding scaled models of trioctyl-TATA are overlaid in Figure 2a,b to illustrate the suggested molecular geometry. There are two possible orientations of the octyl groups with respect to the TATA edge: clockwise (*R*-gauche form) or anticlockwise (*S*-gauche form). Molecules with all three octyl groups in the *R*-gauche form are denoted *RRR*, and their mirror-symmetric counterparts are labeled *SSS*. Both configurations exhibit C_3 symmetry. A survey of many islands revealed that all of the molecules within the core of an island (i.e., those with three nearest neighbors) are either *RRR*- or *SSS*-configured. The island cores therefore are described by the chiral notations *R* and *S* (Figure 2c,d). The cavities surrounded by six molecules are indicated by circular saw blade shapes. The white dashed equilaterals in Figure 2a,b indicate the unit cell of the chiral pattern.

Mechanisms leading to chiral adsorbates are mainly classified into four types:[29] adsorption-induced chirality,[30a−c] oblique arrangements of the molecular axis with respect to lattice directions of the surface or each other,[5a,30d−h] chiral footprints,[30i] and chemical reactions.[30j] The present case may be classified as a chiral footprint, as the interactions between the surface and the octyl group induce the gauche form, which results in chiral adsorbates.

dx.doi.org/10.1021/ja4036187 | J. Am. Chem. Soc. 2013, 135, 8814−8817

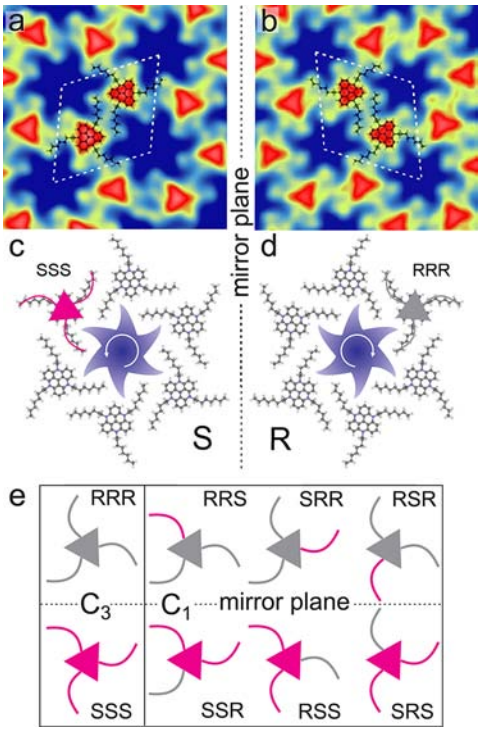

Figure 2. (a, b) STM topographs (7 nm × 7 nm, 100 mV, 100 pA) of homochiral hexagonal patterns with (a) *S* and (b) *R* chiralities. Scaled models are overlaid on the STM topograph. Dashed equilaterals indicate unit cells. (c, d) Models of the (c) *S* and (d) *R* arrangements. Circular saw blade shapes indicate the interior cavities, and circular arrows indicate the conformer chiralities. (e) Possible configurations of the octyl groups in trioctyl-TATA on the surface. For simplicity, triangles with three arcs are used to represent trioctyl-TATA. For an isolated molecule on a perfect plane, some of these configurations (e.g., SSR, SRS, and RSS) are equivalent (they can be superimposed by rotation). However, the local molecular symmetry is perturbed upon absorption on a structured surface such as Au(111). Thus, distinguishable structures ("paramers") may result. This is not the case with our system because the C_3 axes of the TATA molecules happen to coincide with those of the Au(111) surface. However, the symmetry is broken as soon as the interaction with a neighboring molecule is taken into account, resulting in the eight distinct "perimers" shown.[28]

Molecules at the edges of the islands (Figure 1f) may exhibit configurations other than *RRR* or *SSS*. Their octyl groups dangling to the exterior of the island were observed to have the *R*-gauche and *S*-gauche forms with equal probabilities. Figure 3b shows the fraction of C_3-symmetric molecules (*RRR* or *SSS*) in an island on Ag(111). Section S3 in the SI presents an analysis of the fraction of C_3-symmetric molecules in an island on Au(111), which shows the same tendency as on Ag(111). Only the smallest islands exhibited no clear preference for one of the enantiomers.

The observed abundances of C_3-symmetric molecules exceed by far those expected from random combinations of the octyl groups. As discussed below, the octyl groups are likely to flip at room temperature. Thus, each arm may be in an *R*-gauche or *S*-gauche configuration, giving 2^3 possible configurations (Figure 2e) and leading to C_3 and C_1 symmetries. While only four of these configurations are distinct in the gas phase, the others become discernible when neighboring molecules are present on the surface (eight perimers[28]) Only two of the eight combinations are C_3-symmetric, but Figure 3b shows their probability to be ∼3.5 times higher.

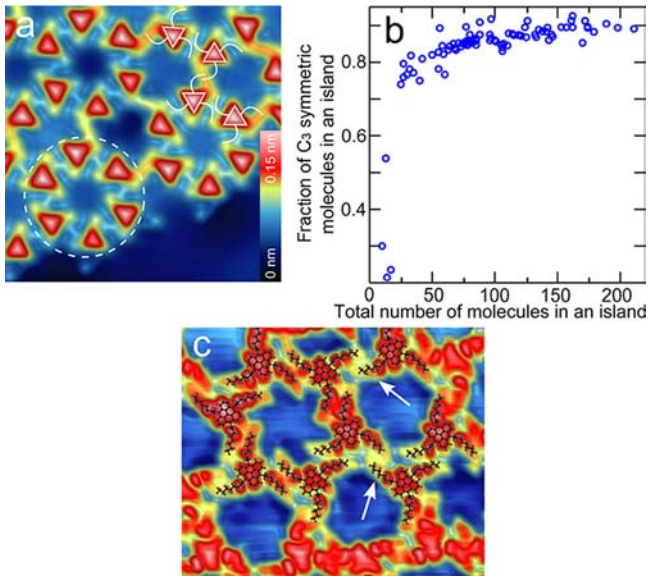

Figure 3. (a) Pseudo-3D-illuminated STM topograph (10.5 nm × 10.5 nm, 10 mV, 10 pA) of a self-assembled island of trioctyl-TATA on Ag(111). (b) Fraction of C_3-symmetric (*RRR* or *SSS*) trioctyl-TATA molecules in an island as a function of island size. (c) High-resolution STM topograph (8.2 nm × 6.7 nm, 1.38 V, 40 pA) of trioctyl-TATA islands on Ag(111) with overlaid molecular sketches scaled to the STM images. The network can be modeled in agreement with the STM images only when all of the octyl groups exhibit the gauche form. The arrows mark positions where the relative orientation of the octyl groups deviates from that observed on Au(111).

We suggest a possible mechanism leading to the observed preference for chiral arrangements of the octyl ligands. The most stable conformation of the octyl groups in the gas phase (Figure 1a,b) is all-anti, with all of the alkyl chains pointing away from the TATA center and the axis of alkyl chain forming an angle of ∼30° with respect to the molecular plane. Because of the large separation of the octyl chains of a given molecule, which essentially prevents them from interacting with each other, the most likely scenario is that the alkyl chains randomly adopt either *R*- or *S*-gauche forms during adsorption. To obtain the observed large excess of C_3-symmetric molecules, flipping between these two forms is required. This involves lifting of an octyl group from the surface and a subsequent rotation around the C2−C3 bond. We propose that this process occurs under the preparation conditions. According to Figure 1e, five of the eight C atoms are in contact with the surface. Lacking the desorption energy of pentane, we used those of butane (∼40.5 kJ/mol[31]) and hexane (∼55.9 kJ/mol[31]) along with the energy barrier for rotation of a C−C bond in butane (∼17 kJ/mol[1]) to estimate the flipping rate and found that flipping of the octyl chains should occur at ambient temperature (section S4 in the SI). When a molecule approaches a chiral island, steric interactions induce a bias in favor of the octyl group orientation matching that of the island, leading to the chiral amplification.

The preference of the gauche form of the octyl groups has an additional consequence for the adlayer structure, namely, the formation of cavities in a honeycomb pattern. One of the octyl groups of each TATA molecule forming a hexagonal ring points toward the cavity. These groups sterically prevent additional molecules from being adsorbed in the cavity.

The results reported for Au(111) are not unique. On Ag(111), we observed a similar symmetry enhancement. Figure 3a shows

dx.doi.org/10.1021/ja4036187 | J. Am. Chem. Soc. 2013, 135, 8814−8817

an STM topograph of an island of trioctyl-TATA on Ag(111) prepared by the same procedure as for Au(111). The packing of the molecular unit cells on Ag(111) deviates somewhat from that on Au(111).[32] However, the same hexagonal pattern is observed (dashed circle in Figure 3a), and the circular saw blade-shaped cavity is clearly discernible. The arrangement of molecules within the hexagonal pattern as extracted from high-resolution STM images (Figure 3c) matches that on Au(111) (Figure 2c,d). As observed on Au(111), all of the core-molecule octyl groups are in the gauche form and all of the island cores are homochiral (*RRR* or *SSS*).

In summary, we have used UHV electrospray deposition and low-temperature STM to obtain detailed images of trioctyl-TATA on Au(111) and Ag(111). The three octyl chains attached to the TATA core are bent because they surprisingly adsorb in gauche form. Hence, the trioctyl-TATA molecules on the surface are chiral. Moreover, preferentially only one of the eight possible perimers[28] is found in homochiral hexagonal networks (chiral amplification).[33,34] There is a dynamic equilibrium between the eight different perimers at room temperature. However, upon attachment to a growing domain, the molecules are actively converted into one of the perimers from which the domain is made up. While chiral amplification on surfaces has been observed before from an equilibrium of two enantiomers,[35] we present the amplification of single enantiomers from four different enantiomeric perimer pairs. Chiral amplification has been proposed as the symmetry-breaking mechanism during the emergence of life.[36] Surface reactions may be particularly effective in symmetry-breaking.[29,30j,37]

■ ASSOCIATED CONTENT

Supporting Information

Procedures and additional results. This material is available free of charge via the Internet at http://pubs.acs.org.

■ AUTHOR INFORMATION

Corresponding Author

gopa@physik.uni-kiel.de

Notes

The authors declare no competing financial interest.

■ ACKNOWLEDGMENTS

Funding by the Deutsche Forschungsgemeinschaft (SFB 677) and the Innovationsfonds Schleswig-Holstein is gratefully acknowledged. STM images were processed using WSxM 5.0.

■ REFERENCES

(1) Wade, L. G. *Organic Chemistry*; Prentice-Hall: Englewood Cliffs, NJ, 1999.

(2) Bartell, L. S.; et al. *J. Chem. Phys.* **1963**, *39*, 3097.

(3) Knippenberg, S.; et al. *J. Chem. Phys.* **2007**, *127*, No. 174306.

(4) Lüttschwager, N. O. B.; et al. *Angew. Chem.* **2013**, *125*, 482.

(5) (a) Charra, F.; et al. *Phys. Rev. Lett.* **1998**, *80*, 1682. (b) Qiu, X.; et al. *J. Am. Chem. Soc.* **2000**, *122*, 5550. (c) Schuurmans, N.; et al. *J. Am. Chem. Soc.* **2004**, *126*, 13884. (d) Nath, K. G.; et al. *J. Am. Chem. Soc.* **2006**, *128*, 4212. (e) Tahara, K.; et al. *J. Am. Chem. Soc.* **2006**, *128*, 16613. (f) Bléger, D.; et al. *Angew. Chem.* **2007**, *119*, 7548. (g) Miyake, K.; et al. *Langmuir* **2008**, *24*, 4708. (h) Lei, S.; et al. *Nano Lett.* **2008**, *8*, 2541. (i) Arrigoni, C.; et al. *J. Phys. Chem. Lett.* **2010**, *1*, 190.

(6) (a) Rabe, J. P.; Buchholz, S. *Science* **1991**, *253*, 424. (b) Hentschke, R.; et al. *J. Chem. Phys.* **1992**, *96*, 6213. (c) Watel, G.; et al. *Surf. Sci.* **1993**, *281*, L297. (d) Marchenko, A.; et al. *Surf. Interface Anal.* **2000**, *30*, 167. (e) Xie, Z.; et al. *Chem. Phys. Lett.* **2000**, *323*, 209.

(7) Yamamoto, M.; et al. *J. Phys. Chem. B* **2000**, *104*, 7363.

(8) Endo, O.; et al. *J. Phys. Chem. B* **2006**, *110*, 13100.

(9) Inga, R.-R.; et al. *Phys. Chem. Chem. Phys.* **2010**, *12*, 4564.

(10) Snyder, R. G.; et al. *J. Chem. Phys.* **1984**, *81*, 5352.

(11) Kanai, K.; et al. *Phys. Chem. Chem. Phys.* **2010**, *12*, 273.

(12) Guo, Z.; et al. *J. Am. Chem. Soc.* **2011**, *133*, 17764.

(13) (a) Yamada, R.; et al. *J. Phys. Chem. B* **2000**, *104*, 6021. (b) Zhang, H.-M.; et al. *Chem.—Eur. J.* **2004**, *10*, 1415. (c) Yang, T.; et al. *J. Chem. Phys.* **2008**, *128*, No. 124709.

(14) Claypool, C. L.; et al. *J. Phys. Chem. B* **1997**, *101*, 5978.

(15) Zhang, H.-M.; et al. *Chem.—Eur. J.* **2006**, *12*, 4006.

(16) Cyr, D. M.; et al. *J. Phys. Chem.* **1996**, *100*, 13747.

(17) (a) Poirier, G. E.; et al. *Langmuir* **1994**, *10*, 2853. (b) Delamarche, E.; et al. *Adv. Mater.* **1996**, *8*, 719. (c) Kondoh, H.; et al. *J. Chem. Phys.* **1999**, *111*, 1175.

(18) Baisch, B.; et al. *J. Am. Chem. Soc.* **2009**, *131*, 442.

(19) Florio, G. M.; et al. *J. Phys. Chem. C* **2008**, *112*, 18067.

(20) (a) Hamann, C.; et al. *Rev. Sci. Instrum.* **2011**, *82*, No. 033903. (b) Hauptmann, N.; et al. *J. Phys. Chem. C* **2013**, *117*, 9734.

(21) Kubitschke, J.; et al. *Eur. J. Org. Chem.* **2010**, 5041.

(22) Weigelt, S.; et al. *J. Am. Chem. Soc.* **2008**, *130*, 5388.

(23) (a) Kuhn, S.; et al. *Phys. Chem. Chem. Phys.* **2010**, *12*, 4481. (b) Jung, U.; et al. *Langmuir* **2011**, *27*, 5899. (c) Jung, U.; et al. *J. Phys. Chem. C* **2012**, *116*, 25943.

(24) Sierka, M.; et al. *J. Chem. Phys.* **2003**, *118*, 9136.

(25) Grimme, S.; et al. *J. Chem. Phys.* **2010**, *132*, No. 154104.

(26) TURBOMOLE V6.2, 2010; a development of University of Karlsruhe and Forschungszentrum Karlsruhe GmbH 1989−2007, TURBOMOLE GmbH since 2007; http://www.turbomole.com.

(27) (a) Müller, T.; et al. *Langmuir* **2003**, *19*, 2812. (b) Yin, S.; et al. *Surf. Interface Anal.* **2001**, *32*, 248.

(28) We introduce the terms "paramer" (Greek *para*, "next to", "along") and "perimer" (Greek *peri*, "around") to adapt the concept of isomers to a surface environment. An adsorbed molecule and a crystalline surface form a complex whose point group may be a subgroup of that of the molecule.[38] Paramers are isomers that emerge from the symmetry reduction of a molecule if the symmetry of the surface is included. Perimers are isomers that emerge from paramers if further symmetry reduction arising from neigboring molecules is considered.

(29) Ernst, K.-H. *Phys. Status Solidi B* **2012**, *249*, 2057.

(30) (a) Böhringer, M.; et al. *Phys. Rev. Lett.* **1999**, *83*, 324. (b) Böhringer, M.; et al. *Angew. Chem., Int. Ed.* **1999**, *38*, 821. (c) Böhringer, M.; et al. *Angew. Chem., Int. Ed.* **2000**, *39*, 792. (d) Kuntze, J.; et al. *Nanotechnology* **2004**, *15*, S337. (e) Richardson, N. V. *New J. Phys.* **2007**, *9*, 395. (f) Jiang, N.; et al. *Phys. Chem. Chem. Phys.* **2010**, *12*, 1318. (g) Mugarza, A.; et al. *Phys. Rev. Lett.* **2010**, *105*, No. 115702. (h) Gopakumar, T. G.; et al. *J. Phys. Chem. C* **2010**, *114*, 18247. (i) Humblot, V.; et al. *J. Am. Chem. Soc.* **2004**, *126*, 6460. (j) Messina, P.; et al. *J. Am. Chem. Soc.* **2002**, *124*, 14000.

(31) Wetterer, S. M.; et al. *J. Phys. Chem. B* **1998**, *102*, 9266.

(32) At present, the reason for this difference is not clear. The herringbone reconstruction of Au(111), which does not occur on Ag(111), was observed to persist underneath molecular islands. However, it does not significantly affect the growth directions of the islands and thus appears to be unimportant here. Other differences between Ag and Au (e.g., the small difference in lattice constants or different surface-state energies) may be involved.

(33) Siegwarth, J.; et al. *Org. Lett.* **2009**, *11*, 3450.

(34) Ernst, K.-H. *Origins Life Evol. Biospheres* **2010**, *40*, 41.

(35) Weigelt, S.; et al. *Nat. Mater.* **2006**, *5*, 112.

(36) Mason, S. F. *Int. Rev. Phys. Chem.* **1983**, *3*, 217.

(37) (a) Hwang, Y. J.; et al. *J. Am. Chem. Soc.* **2005**, *127*, 5016. (b) Lopinski, G. P.; et al. *Nature* **1998**, *392*, 909. (c) Kahr, B.; et al. *Chirality* **2008**, *20*, 973. (d) Zepik, H. *Science* **2002**, *295*, 1266.

(38) Nichols, H.; et al. *J. Chem. Phys.* **1981**, *75*, 3126.